Microporous Carbon adsorbents with high CO_2 capacities for industrial applications

Santiago Builes,[a,b] Thomas Roussel,*[b] Camelia Matei Ghimbeu,[c] Julien Parmentier,[c] Roger Gadiou,[c] Cathie Vix-Guterl[c] and Lourdes F. Vega[a,b]

Supplementary Information

Details about the carbon model structures:

As the focus of this contribution is in the application of zeolite template carbons (ZTC) to CO2 adsorption, rather than the development of a molecular model for the materials we do not report this information in the body of the paper. The methodology to numerically synthesize these model materials, and the structural and mechanical characteristics of both models used for this work can be found in the literature. (Roussel *et al. J. Phys. Chem. C* **2007**, *111*, 15863 and Roussel *et al. J. Chem. Phys.* **2009**, *130*, 174717).

For completeness we present here the basic details about the computational synthesis and the structure of the modelled materials. The atomistic carbon structures of the hexagonal (EMT) and cubic (FAU-Y) faujasite zeolite carbon replicas were obtained using the standard Grand Canonical Monte Carlo (GCMC) method. Simulations were performed on a periodic simulation box containing a unit cell of cubic faujasite zeolite FAU (~24.85 Å), and the smallest orthorhombic unit cell of the hexagonal faujasite EMT (corresponding to two hexagonal unit cells in <x,y> directions: a_x = 17.386 Å , a_y = 30.114 Å and a_z = 28.346 Å). Starting with a C_2 dimer, the chemical potential was raised exploring the accessible space of configurations in the system. The carbon-carbon interactions were described with the bond order potential of Stuart-Brenner-Tersoff (AI-REBO)[1]. The Pellenq-Nicholson-Transferable to All Zeolite interatomic potential (PN-TrAZ) was used for the interactions between carbon and zeolite species (Al, Si and O)[3].

The negative templated structures, formed when zeolite voids are filled out of carbon atoms, consisted of cages delimited by tubular walls; these walls are made of carbon atoms in their sp^2 hybridization state. The extreme curvature of the templated carbon is stabilized by the presence of five and seven member rings. The proportions of 6-member rings are on the order of 60 % and 40% shared by 5, 7 and some 8-member rings. These structures do not have dangling bonds or sp^3 carbon atoms, and represent two very stable (-7.2 eV/at) and degenerate states with possible phase coexistence. Their densities, respectively 0.81 and 0.96 g/cc for the FAU and EMT, correspond to the carbon weight over the total volume of the simulation boxes.

As explained in the text, these simulated materials capture the structure of the experimental material, as well as key features of them; however, one should bear in mind that this is a quite simple and rude model, highly ideal, and hence, some features and defects of the experimental material may not show up into the model.

Nitrogen adsorption:

We present here the adsorption isotherms of nitrogen (N_2) at 77K. The simulations with N_2 aim to prove the hypotheses made in this paper for CO_2 adsorption on Zeolite Templated Carbon (ZTCs). The simulations with N_2 show interesting features about the microstructures of ZTCs. We followed the same simulation techniques than for CO_2 (explained in the body of the paper) and provide the parameters at the end of this section. The use of this other probe gas aims to provide more information on the structure of these materials, and, in particular, on the effect of extreme curvature in the case of FAU-ZTCs, and on the presence of the small cages in the case of EMT-ZTCs already observed for CO_2. Nitrogen is also used to calculate the microporous volume of the structure models, defined as the void accessible volume left after subtracting the volume occupied by the solid, which includes the Connoly surface. The results of the adsorption isotherms are shown bellow (Figure S1). The structure models densities reported in the manuscript correspond to the carbon masse per volume occupied by the carbon framework in the total volume of one un cell.

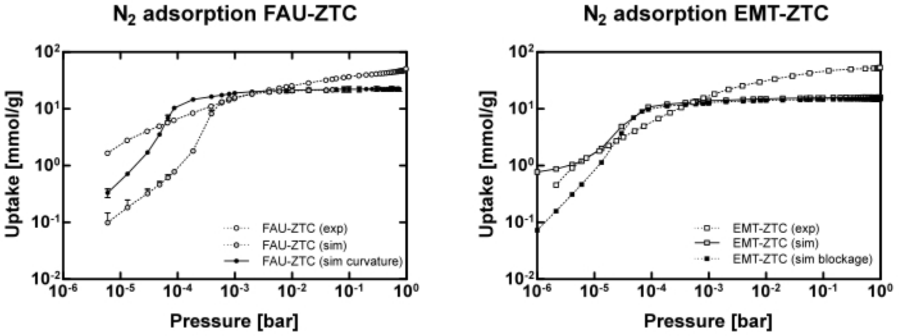

Figure S1. Adsorption isotherms for N_2 in FAU-ZTC (*left*) and EMT-ZTC (*right*) for experimental results (*open symbols*), simulated isotherms (*gray symbols*) and corrected simulated isotherms using the two different bias (*filled symbols*).

The pressure range of the simulations was adjusted to correspond to the experimental data. The conclusions obtained from N_2 adsorption data are not directly extendable to the case of CO_2, given that the coverage of N_2 varies much more quickly. Indeed, experimentally, a very high uptake of N_2 is already achieved at very low pressure (*i.e.* ~ 1 mmol/g at $P < 10^{-5}$ bar), which does not allow obtaining data with nitrogen at very low coverage. Therefore, in order to distinguish different sizes of micropores present in the material, it is necessary to collect data at lower pressures or higher temperature using nitrogen, or other probe molecules.

In both cases, experimental and simulated curves behave similarly (for the limited range we can compare). For comparison, the adsorption isotherms of N_2 at 77K and CO_2 at 273K for FAU-ZTCs are shown in Figure S2, while Figure S3 shows them for EMT-ZTCs.

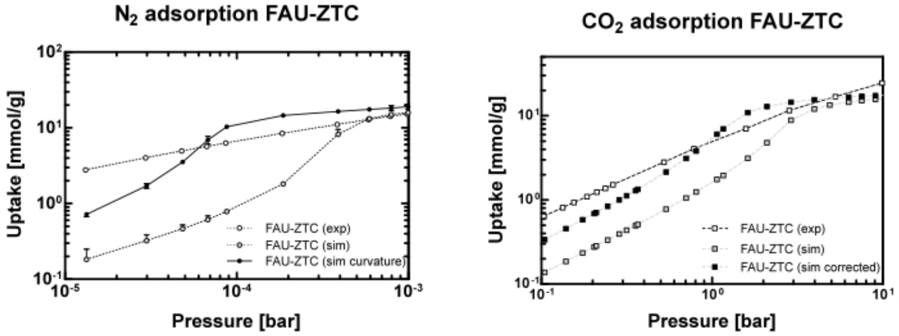

Figure S2. Adsorption isotherms for FAU-ZTC for N_2 at 77K (*left*) and CO_2 at 273K (*right*)

Several comments are in order here: first, in the case of FAU-ZTCs, the experimental adsorption values are higher than the simulated ones for both probe molecules (N_2 and CO_2), even if the curvature effects are included in the simulations. In this latter case, we observe a crossover at ~ $6x10^{-5}$ bar for nitrogen, and ~ 0.8 bar for carbon dioxide. These crossovers correspond to an inflection point in the simulated isotherms, meaning that the fluid starts to compress because of the limited accessible volume already filled in the models, while extra room is accessible in the real material. We observe the same behaviour without taking into account curvature effects, and reach the same uptake at pressures of 10^{-3} bar and 6 bar, respectively, for nitrogen and carbon dioxide.

This partially confirms that the curvature effect drastically affects the amount adsorbed. Probably the overestimated density of the model structure would provide another drastic change in the amount adsorbed, but it would not change the slope of the isotherm. Other effects are missing in the model. For instance, smaller pores due to eventual collapsed microstructures (see figure S4), or hetero-species present from the organic precursors, or else the presence of localized partial charges on the carbon structure would adjust better the slope of the experimental isotherm at very low coverage. These latter aspects are under consideration for further improvements of the model.

The adsorption isotherms of N_2 at 77K and CO_2 at 273K for EMT-ZTC are depicted in Figure S3. Herein, we again consider only the effect of the accessibility of the cages formed by the carbon pillars.

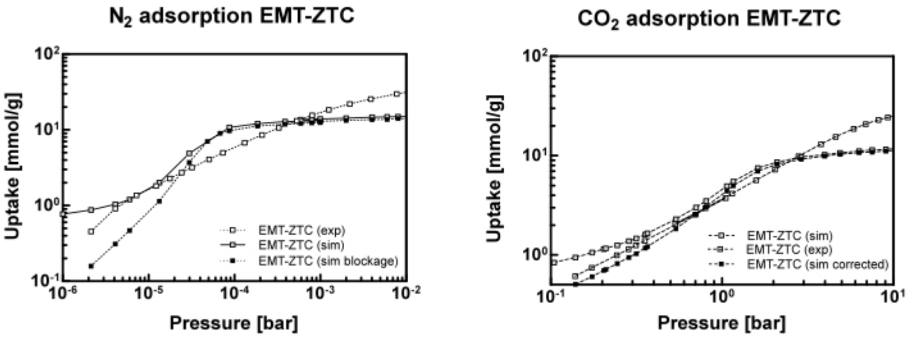

Figure S3. Adsorption isotherms for FAU-ZTC for N_2 at 77K (left) and CO_2 at 273K (right)

The isotherms can be divided in two regions:

1 - Above 10^{-4} bar for nitrogen and 1 bar for CO_2: in this region we observe a change in the slope of the simulated adsorption isotherms due to the microporosity being already filled out; it results in the compression of the fluid, while experimentally the materials can still adsorb more molecules in larger pores. Therefore, the model made only of carbon micropores get saturated at coverage about 10 mmol/g.

2 - Low relative pressures, *i.e.* $[10^{-6}:2x10^{-5}]$ bar in the case of nitrogen and $[10^{-1}:1]$ bar for CO_2: we have already shown that in this range of pressure, the inclusion of CO_2 in the cages leads to an overestimation of the uptake, and their exclusion correctly predicts the slope of the adsorption isotherm at 273K from very low pressure until saturation of the accessible volume in the model.

It is interesting to observe the opposite behaviour in the case of nitrogen at 77K. Indeed, if N_2 can access to the pillared cages, the simulated isotherm is then in perfect agreement with the experiment in this first low pressure range. This new insight of the EMT-ZTCs microstructure reinforces the first assumption, and a criterion to eventually identify the presence of a tubular pillared structure.

Another major point that can be extracted from the nitrogen data is that it is possible to characterise and distinguish the presence of different small micropores very close in size using two different probes at different thermodynamic conditions. This is especially important in the case of multimodal microporous materials with complex textural properties.

The nitrogen adsorption isotherms have been used to obtain the Pore Size Distribution (PSD) of the experimental and modelled materials.

Pore Size Distributions:

The Pore Size Distributions (PSDs) of the model structure obtained numerically are presented in Figure S4. To help with the comparison, the PSDs were normalized respect to their integrals, and magnified 10 times for the experimental curves. The experimental PSD were calculated using the NLDFT method from nitrogen physisorption data at 77K (*circles*) while the simulated were obtained using the Monte-Carlo scheme of Gelb and Gubbins with nitrogen as the probe molecule (*squares*).

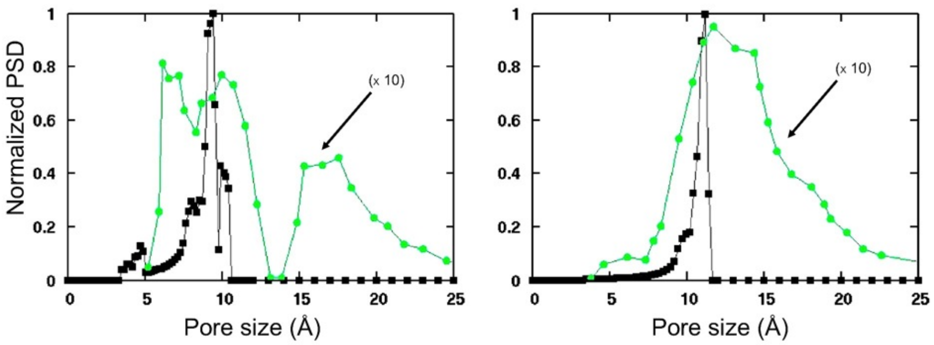

Figure S4: PSD comparisons for the experimental (*green circles*) and the simulated (*black squares*) EMT-ZTCs (*left*) and FAU-ZTCs (*right*).

Although both PSD show a pick at about the same size, the PSD obtained with the experimental data are broader than those obtained with the simulation data and the simulated structure. Assuming a maximized carbon loading and considering the statistical mechanics approach used to obtain the most stable negative structure of the hosts, the real materials have either several defects, or heteroatoms from the organic precursor, or else cavities and edges corresponding to the size of the unit cells of the zeolites. This yields to non-negligible microporosity differences, with pore sizes greater than the zeolite wall thickness, and even of the size of the host unit cell dimensions. Also, the presence of smaller micropores in the experimental PSD could also be due to partial microstructure collapsing. These discrepancies found in the PSD imply differences in terms of micropore volumes, surface area, and densities and also explain most of the adsorption isotherms different behaviours.

[1] Brenner, D.W.; Shenderova, O.A.; Harrison, J.A.; Stuart, S.J.; Ni, B.; Sinnott, S.B. *J. Phys.: Condens. Matter* **2002**, *14*, 783

[2] Pellenq, R. J. M.; Nicholson, D. *J. Phys. Chem.* **1994**, *98*, 13339

X-ray diffraction analysis:

Using the Reflex module in the Materials Studio software the Powder Crystallinity was determined. This helps probing for the presence of mixtures of different crystalline and amorphous phases. In order to determine the degree of crystallinity, the program needs to deconvolute the X-ray data into three scattering contributions: crystalline, amorphous, and background. The background contribution represents the background noise and is removed from the calculation; then, the degree of crystallinity is determined from the area difference between the crystalline and amorphous contributions

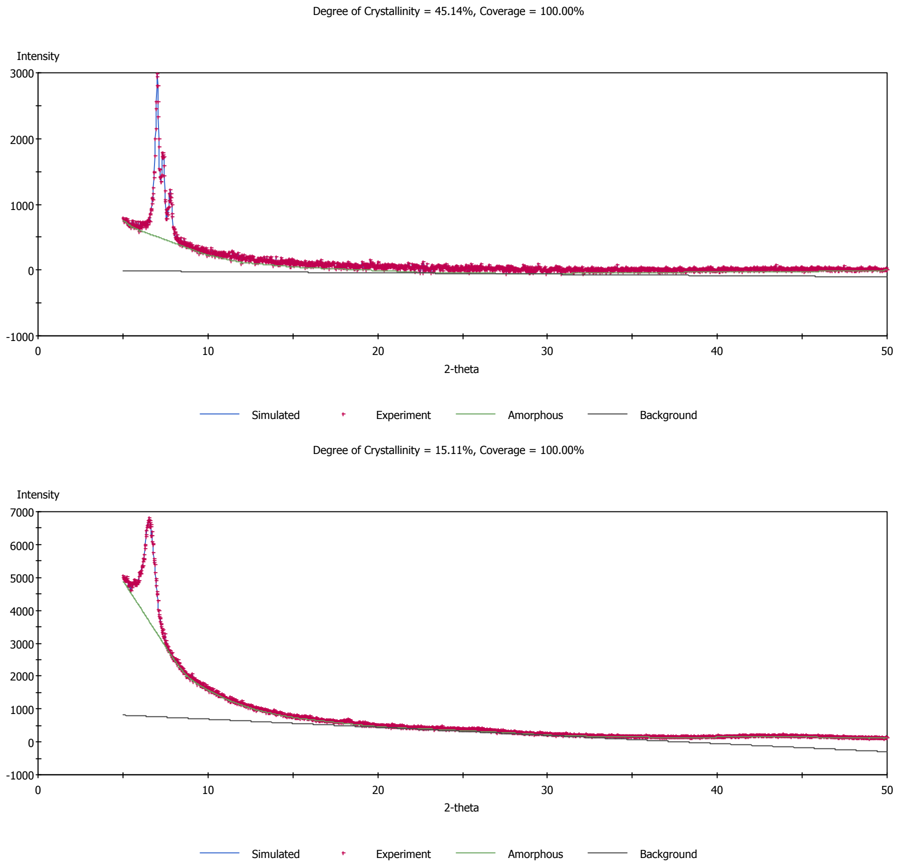

Figure S5: X-ray diffraction of the samples used to determine the degree of crystallinity of the EMT-ZTC (top) and FAU-ZTC (bottom) samples.

Using the Reflex module it is possible to remove the background and smooth from the experimental samples. This data can be compared to the XRD from the models generated using the same program. The XRD from the models can be refined to account for a finite particle-size contribution to the measured peak widths adjusting the crystallite size; this means that the crystallites constituting the powder sample are small (less than 1000 Å) there will be a finite particle-size contribution to the measured peak widths. Figure S6 shows a comparison of the resulting XRD for the treated samples (background removed) and the models (refining automatically their crystallite size).

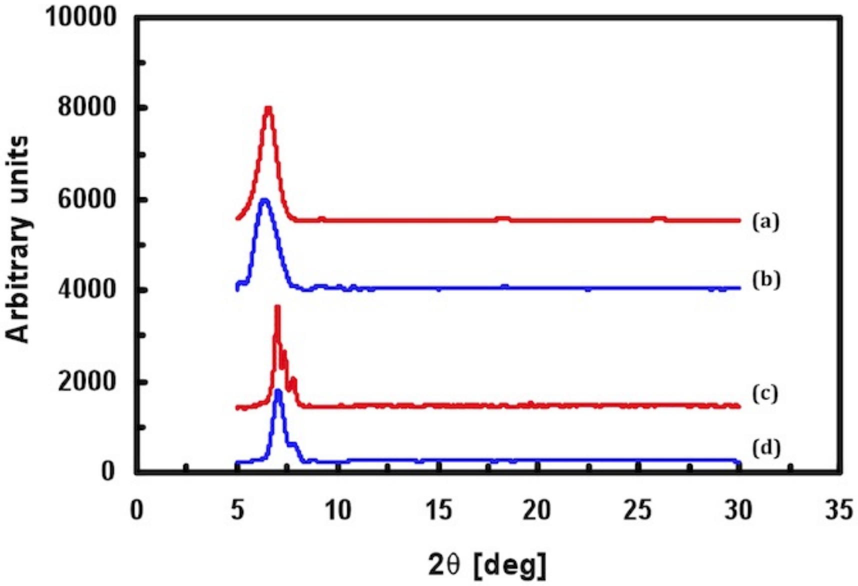

Figure S6: XRD of the experimental samples EMT-ZTC (a) and FAU-ZTC (c) and of their corresponding models (b and d).